were measured at pressures of 515 and 715 psia. A slope of 1.14 and intercept of −430 lb-sec/in.[3] were obtained from a straight line fit of the data. Figure 2 shows the results obtained from four mixes with different blends of three oxidizer grinds. Burning rates were measured at pressures of 315, 515, and 715 psia. A straight line through the data gave a slope of 1.14 and intercept of −550 lb-sec/in.[3].

The slopes and intercepts for fits of small motor and liquid strand data to Eq. (1) have been measured for both polyurethane and polybutadiene formulations. Data precision of 2% or better has resulted. The observed scatter has been largely attributable to the small motors. Formulations not containing burning-rate catalyst have yielded slopes ranging between 1.12 and 1.18, with intercepts ranging between −350 and −550 lb-sec/in.[3]. Therefore, the trends predicted by the Summerfield Granular Diffusion Model have been verified experimentally. More economical motor design through increased application of strand burning rates can be achieved through the use of Eq. (1).

References

[1] Summerfield, M., Sutherland, G. S., Webb, M. J., Taback, H. J., and Hall, K. P., "Burning mechanism of ammonium perchlorate propellants," *ARS Progress in Astronautics and Rocketry: Solid Propellant Rocket Research*, edited by M. Summerfield (Academic Press, New York, 1960), Vol. 1, pp. 141–160.

[2] Blair, D. W., Bastress, E. K., Hermance, L. E., Hall, K. P., and Summerfield, M., "Some research problems in the steady state burning of composite solid propellants," *ARS Progress in Astronautics and Rocketry: Solid Propellant Rocket Research*, edited by M. Summerfield (Academic Press, New York, 1960), Vol. 1, pp. 183–206.

[3] McCarty, K. P., "Techniques for studying the combustion of aluminum in solid propellant," Pyrodynamics **1**, no. 1, 71–87 (1964).

Electric Propulsion Characteristics of a Pulsed Plasma Rail Accelerator

Daniel H. Winicur*
Hughes Aircraft Company, El Segundo, Calif.

Nomenclature

x = axial displacement of plasma slug
t = time
l = rail electrode length
$2r$ = rail electrode width
d = distance to one rail electrode from centerline of the other rail electrode
I = electric current
V = voltage
C = capacitance
R = resistance
L = inductance
B = magnetic field along the plasma slug caused by the current flowing in the rail conductors
v = plasma velocity
m = mass per pulse
T = discharge time
g_0 = gravity constant
μ_0 = magnetic permeability of a vacuum
F = instantaneous force on plasma slug
E = stored energy per plasma slug mass
s = total length of plasma column
ds = increment of plasma column length
K = magnetic field strength per unit current acting on plasma
I_T = total impulse per pulse
I_{sp} = specific impulse
Pe = accelerator jet power
(P/F) = specific power
η = power efficiency
ΔV = net velocity increment

Subscript

0 = power supply circuit element

Superscripts

$(\ )'$ = value per unit or rail length
$(\bar{\ })$ = averaged quantity

Received October 14, 1963; revision received May 22, 1964.
* Member of the Technical Staff, Space Systems Division. Associate Member AIAA.

THIS note presents the results of an analog computer study of the electric propulsion characteristics of a confined pulsed plasma rail accelerator. The rail accelerator has been proposed for long duration space propulsion missions such as attitude control, orbit raising, and deep space propulsion.[1–3] The theory and operation of this accelerator is amply described in Refs. 1–6.

The "plasma slug model" has been used with variable rail resistance and inductance. The propellant is assumed to be injected in a compact form with the plasma remaining as a slug. This plasma slug is then treated as a moving circuit element of negligible resistance.[3] Assuming that the motion of the plasma slug can be described one-dimensionally,

$$dL/dt = (dL/dx)(dx/dt) = L'v \tag{1}$$

where dL/dx is assumed to be a constant equal to L', the rail inductance per unit length.

Starting with the expression for the instantaneous force on a column of plasma moving in a direction normal to the current flowing through it,

$$F = I\int_s B\,ds \tag{2}$$

Maes[1] has derived the following equation for F which includes the force due to the current flowing in the back conductors, parallel to the plasma slug, in addition to the force due to the current flowing through the parallel rail electrodes:

$$F = -\frac{\mu_0 I^2}{2\pi}\left\{\frac{(x^2+d^2)^{1/2}}{x} + \ln\left[\frac{x+(r^2+x^2)^{1/2}}{x+(d^2+x^2)^{1/2}}\right] + \ln\frac{d}{r} - 1\right\} \tag{3}$$

When $x \gg d$, i.e., when the effect of the back conductors is negligible, this reduces to the familiar expression

$$F = \tfrac{1}{2}L'I^2 \tag{4}$$

After integrating Eq. (3) from $x = 0$ to $x = l$ to obtain the space average of F, the instantaneous force on the plasma can be expressed as

$$F = KI^2 \tag{5}$$

The coefficient K is a constant dependent only on the accelerator geometry equal to the magnetic field strength per unit current acting on the plasma column.

The time varying resistance and inductance are then expressed in terms of R' and L':

$$R = R'x \qquad L = L'x \tag{6}$$

Equation (5) is combined with the Kirchhoff voltage equation of the equivalent electrical current to yield the equation governing the current flowing in the rails:

$$0 = \frac{1}{C_0}\int_0^t I\,dt + \left[L_0 + \frac{L'K}{m}\int_0^t\int_0^t I^2 dt\,dt\right]\frac{dI}{dt} + I\left[R_0 + \frac{R'K}{m}\int_0^t\int_0^t I^2 dt\,dt + \frac{L'K}{m}\int_0^t I^2 dt\right] \tag{7}$$

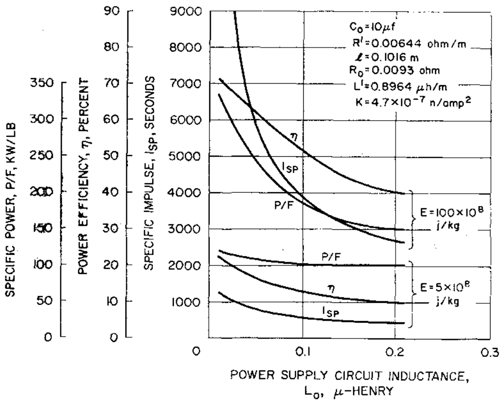

Fig. 1 Specific power, power efficiency, and specific impulse vs power supply circuit inductance.

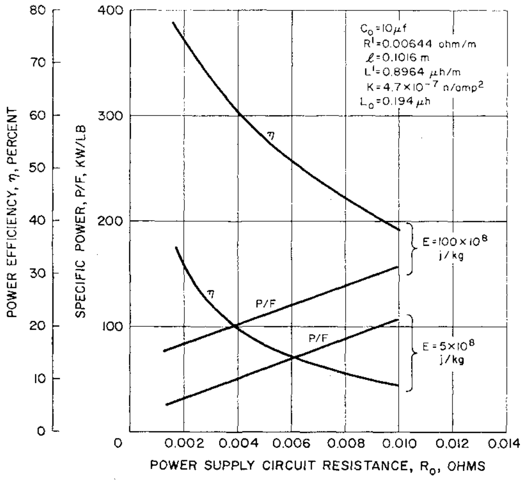

Fig. 2 Power efficiency and specific power vs power supply circuit resistance.

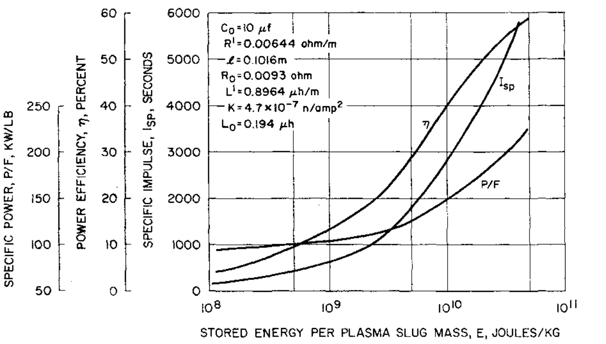

Fig. 3 Specific power, power efficiency, and specific impulse vs stored energy per plasma slug mass.

The propulsion parameters (average thrust $\bar{F}$, total impulse per pulse I_T, specific impulse I_{sp}, accelerator jet power Pe, specific power P/F, power efficiency η, and ΔV) were then expressed in terms of the current, and analog computer solutions were obtained for various values of V_0, m, R_0, L_0, and C_0. The values used for K, R', L', and l were obtained from an experimental rail accelerator being built at the Hughes Aircraft Company.

For a given charging voltage V_0, the current does not appear to change appreciably as m is varied. As V_0 increases, the maximum current increases, but the period remains the same. When m is decreased, the discharge time T decreases exponentially.

The effect of reducing L_0 and R_0, on the specific power, specific impulse and efficiency, is shown in Figs. 1 and 2. Reducing L_0 also increases the maximum current and reduces T. This is as expected since the electrical energy initially stored in the power supply capacitor is divided between the magnetic field of L_0 (wasted) and the useful magnetic field between the rails. As L_0 is decreased, an increasingly large percentage of this energy becomes available for accelerating the plasma slug. Decreasing R_0 has a negligible effect on I, F, T, and I_{sp}. However, the power that must be supplied to replace heat dissipation is proportional to R_0, so reducing R_0

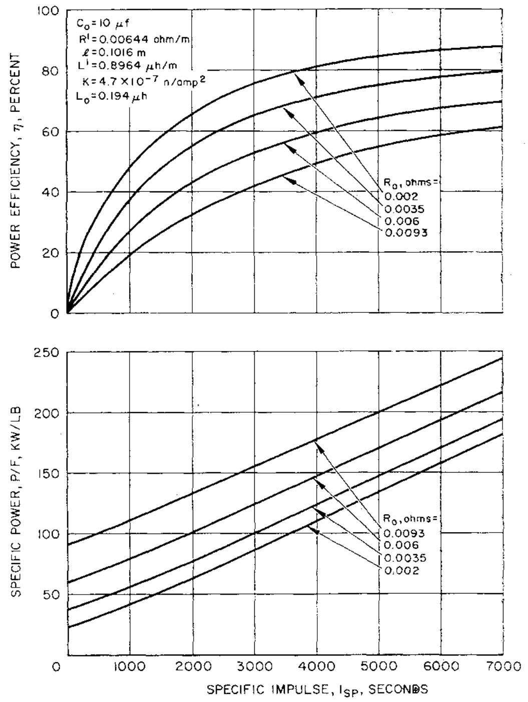

Fig. 4 Power efficiency and specific power vs specific impulse.

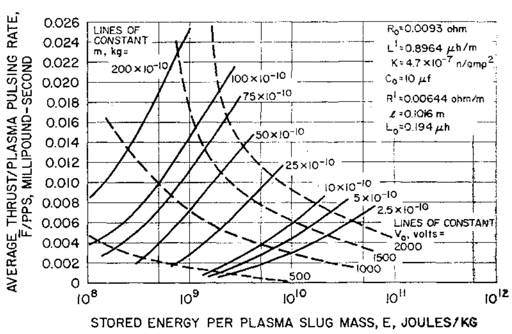

Fig. 5 Average thrust/plasma pulsing rate and average jet power/plasma pulsing rate vs stored energy per plasma slug mass.

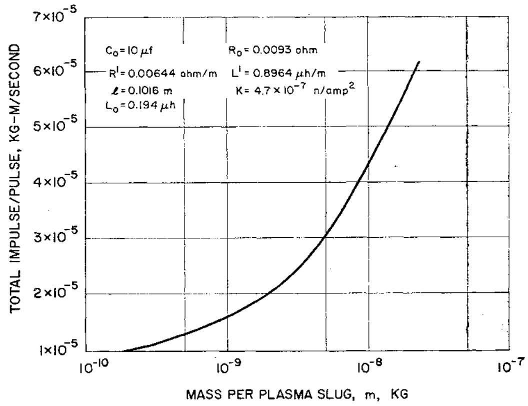

Fig. 6 Total impulse per pulse vs mass per plasma slug.

has the effect of reducing the electrical power input for a given output, thereby raising the efficiency and lowering the specific power.

The specific impulse, specific power, and power efficiency are all functions of the stored energy per plasma slug mass E and are shown in Fig. 3. The relations between η and I_{sp} and P/F and I_{sp} are shown in Fig. 4. The effect of reducing R_0 is seen here to be very marked. The relations between η, P/F, and I_{sp} do not vary with L_0.

The average thrust is shown in Fig. 5 as a function of E. For a constant V_0, $\bar{F}$ increases with increasing m (decreasing E), and, for a constant m, $\bar{F}$ increases with V_0 (increasing E). Since η increases with increasing E, the most advantageous method of increasing the average thrust during operation is to increase the charging voltage.

The total impulse per pulse, equal to ΔV multiplied by the total space vehicle mass, is a linear function of the electrical power input. It is a more complex function of m, as is seen in Fig. 6.

On the basis of these results, the rail accelerator appears to be useful for propulsion in space. The range of operation, where the efficiency is neither too low nor the specific power too high, appears to lie between 1500 and 5000-sec I_{sp}. The rail accelerator has the distinct advantage that one engine can be operated at various points in this range.

References

[1] Maes, M. E., "The confined parallel rail pulsed plasma accelerator," ARS Preprint 2397062 (1962).

[2] "The application of the pulsed plasma accelerator to satellite attitude control," Rocket Research Corp., 62-R-7 (June 1962).

[3] Schock, A., "Electromagnetic acceleration of plasma for space propulsion," *Proceedings of the Fourth AFBMD/STL Symposium* (Pergamon Press, Ltd., London, 1961), Vol. 2, pp. 133–144.

[4] Bostick, W. H., "Plasma motors: The propulsion of plasma by magnetic means," *IX International Astronautical Congress* (Springer-Verlag, Wein, 1959), p. 794 ff.

[5] Thourson, T. L., "Pulsed plasma accelerator," Second Symposium on Advanced Propulsion Concepts (1959), Vol. 1, pp. 73–87.

[6] Mostov, P. M., Neuringer, J. L., Rigney, D. S., "Electromagnetic acceleration of a plasma slug," Phys. Fluids, **4**, 1097–1104 (1961).

Technical Comments

Comments on "Transition Correlations for Hypersonic Wakes"

John I. Erdos* and Harris Gold†

Avco Corporation, Wilmington, Mass.

In a recent note,[1] Zeiberg has shown that the effects of body shape can be removed from a correlation of wind tunnel and ballistics range wake-transition data for various two-dimensional and axisymmetric models by using the Reynolds number based on freestream properties and the distance from the model base to the transition location, a "body bluntness" parameter, and the freestream Mach number. The authors have correlated the same small-scale data[2,3] as have many others,[4–6] each interpreting the results in a different manner but all having essentially the same goals, namely, to understand the phenomenon and to derive a simple formula for the prediction of wake transition for full-scale hypersonic re-entry conditions. Although a correlation such as suggested by Zeiberg, which employs concepts carried over from successful boundary-layer and free-shear-layer transition correlations, does in fact satisfy the latter goal, it contains implications that are contrary to the present understanding of the phenomenon, and its use to predict transition at conditions outside the range of small-scale experimental conditions is certainly questionable.

It is well established that the distance to transition in the wake is a function of the local Mach number and "some" Reynolds number (almost any will correlate the data for a given model). A close scrutiny of the small-scale data at a given freestream Mach number and model shape reveals the behavior sketched in Fig. 1.[4,5] The concept of a unique transition Reynolds number ($\rho_e U_e x_{TR}/\mu_e$) appears to be valid only within a limited range of body Reynolds numbers and/or unit Reynolds numbers (see Table 1). At lower body Reynolds numbers, the transition distance moves out rapidly toward infinity (which has been explained by Lees[4] on the basis of energy arguments), whereas at very high body Reynolds numbers, the transition distance "slows down" as it

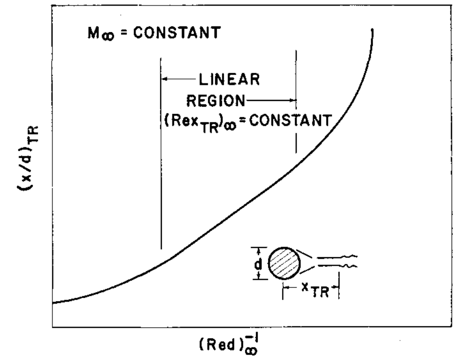

Fig. 1 Schematic representation of wake transition distance vs freestream Reynolds number.

Received May 11, 1964.

* Senior Scientist, Research and Advanced Development Division. Member AIAA.

† Staff Scientist, Research and Advanced Development Division. Member AIAA.